Enhanced formation of fine particulate nitrate at a rural site on the North China Plain in summer: The important roles of ammonia and ozone

Liang Wen [a], Jianmin Chen [a, b, c], Lingxiao Yang [a, b, *], Xinfeng Wang [a], Caihong Xu [a], Xiao Sui [a], Lan Yao [a], Yanhong Zhu [a], Junmei Zhang [a], Tong Zhu [d], Wenxing Wang [a]

[a] Environment Research Institute, Shandong University, Jinan 250100, China
[b] School of Environmental Science and Engineering, Shandong University, Jinan 250100, China
[c] Shanghai Key Laboratory of Atmospheric Particle Pollution and Prevention (LAP3), Fudan Tyndall Centre, Department of Environmental Science and Engineering, Fudan University, Shanghai 200433, China
[d] State Key Lab for Environment Simulation and Pollution Control, College of Environmental Sciences and Engineering, Peking University, Beijing 100871, China

HIGHLIGHTS

- High concentration of nitrate in $PM_{2.5}$ was observed at a rural site in North China.
- High ammonia in the early morning accelerated the formation of fine nitrates.
- The formation of nitrates at night was mainly attributed to the hydrolysis of N_2O_5.

ARTICLE INFO

ABSTRACT

Severe $PM_{2.5}$ pollution was observed frequently on the North China Plain, and nitrate contributed a large fraction of the elevated $PM_{2.5}$ concentrations. To obtain a comprehensive understanding of the formation pathways of these fine particulate nitrate and the key factors that affect these pathways, field measurements of fine particulate nitrate and related air pollutants were made at a rural site on the North China Plain in the summer of 2013. Extremely high concentrations of fine particulate nitrate were frequently observed at night and in the early morning. The maximum hourly concentration of fine particulate nitrate reached 87.2 $\mu g\ m^{-3}$. This concentration accounted for 29.9% of the $PM_{2.5}$. The very high NH_3 concentration in the early morning significantly accelerated the formation of fine particulate nitrate, as indicated by the concurrent appearance of NH_3 and NO_3^- concentration peaks and a rising neutralization ratio (the equivalent ratio of NH_4^+ to the sum of SO_4^{2-} and NO_3^-). On a number of other episode days, strong photochemical activity during daytime led to high concentrations of O_3 at night. The fast secondary formation of fine particulate nitrate was mainly attributed to the hydrolysis of N_2O_5, which was produced from O_3 and NO_2. Considering the important roles of NH_3 and O_3 in fine particulate nitrate formation, we suggest the control of NH_3 emissions and photochemical pollution to address the high levels of fine particulate nitrate and the severe $PM_{2.5}$ pollution on the North China Plain.

© 2014 Elsevier Ltd. All rights reserved.

1. Introduction

Particulate nitrate account for a large fraction of the $PM_{2.5}$ in rural, suburban, urban and industrial areas, usually averagely ranging from 4.5 to 25 % (Ye et al., 2003; Wang et al., 2005; Pathak et al., 2009; Du et al., 2011; Squizzato et al., 2012). Nitrate aerosols can have a stronger impact on visibility than sulphate aerosols in the same concentrations (Lei and Wuebbles, 2013) because the

* Corresponding author. Environment Research Institute, Shandong University, Jinan 250100, China.
E-mail address: yanglingxiao@sdu.edu.cn (L. Yang).

scattering albedo of nitrate aerosols is larger than that of sulphate aerosols in low RH conditions (Zhang et al., 2012). High concentrations of secondary nitrate, sulphate, and organic aerosols have led to frequent haze episodes in North China (Guo et al., 2010; Gao et al., 2011; Wang et al., 2014a,b).

Fine particulate nitrate can be formed through the homogeneous reaction of gaseous HNO_3 and NH_3 (Feng and Penner, 2007). HNO_3 is primarily produced from the reaction between NO_2 and OH radicals during the daytime (Calvert and Stockwell, 1983) and later combines with NH_3 to produce fine particles of NH_4NO_3. Field observations in urban Shanghai show that NH_3 can neutralize HNO_3 in the gas phase and liquid phase, playing a vital role in the increase in particulate nitrate during haze episodes (Ye et al., 2011). NH_4NO_3 aerosols are unstable under conditions of high temperature and low humidity due to the reversible phase equilibrium with HNO_3 and NH_3 (Mozurkewich, 1993). Laboratory studies have shown that low temperature and high RH favoured the formation of nitrate aerosols (Hu et al., 2011; Shi et al., 2014).

In addition, a large fraction of fine particulate nitrate can be produced via the heterogeneous hydrolysis of N_2O_5 on the wet surface of aerosols in the dark (Ravishankara, 1997). N_2O_5 primarily accumulates at night-time via the reversible reaction between the NO_2 and NO_3 radicals which are produced from the reaction of NO_2 with O_3 (Mentel et al., 1996). Several finding shave indicated that strong photochemical activity and high levels of NO_2 promoted the formation of fine particulate nitrate during the night-time (Wang et al., 2009). At a site downwind of Beijing in summertime, the contribution of N_2O_5 hydrolysis to the enhancement of fine particulate nitrate was estimated at up to 50 %–100 % by using a thermodynamic model (Pathak et al., 2009, 2011).

North China, one of the major agricultural and industrial bases, is densely populated and suffered from serious particulate matter pollution and photochemical pollution in the last decade (Wang et al., 2006, 2010; Guo et al., 2010; Luo et al., 2013). Large amounts of NO_x and NH_3 were emitted from industry, vehicles, agriculture, and daily activities on the North China Plain (Meng et al., 2010; Shen et al., 2011; Carslaw and Rhys-Tyler, 2013). In recent years, the NO_x emissions have kept rising because of the continuous increase in the number of motor vehicles (Richter et al., 2005; Liu et al., 2013). Consequently, both the concentration of fine

particulate nitrate and the fraction of fine particles containing nitrate show an increasing trend (Lei and Wuebbles, 2013).

In this study, intensive field measurements, including $PM_{2.5}$, fine particulate nitrate and other water-soluble ions, aerosol surface area, trace gases and meteorological parameters, were conducted at a rural site in the middle of the North China Plain from June 18 to June 30, 2013. Surprisingly, extremely high concentrations of fine particulate nitrate and fast nitrate formation were observed. The dominant formation pathways of the elevated fine particulate nitrate were analysed in detail based on real-time observations in combination with numerical calculations.

2. Experiments and methods

2.1. Sampling site

The measurement site of this study was located in rural Yucheng, Dezhou, Shandong Province, China (36.87°N, 116.57°E, ~23 m a.s.l.), which is almost in the centre of the North China Plain (as shown in Fig. 1). The selected site was in an open field surrounded by farmland. Yucheng and the surrounding areas are famous for their agriculture (e.g., wheat and corn) and grazing land (e.g., donkeys and chickens). In addition, the site near 20 to 30 Km radius located several factories in the production of inorganic and organic fertilizers. These, in addition to the application of fertilisers to farmland emitted a great deal of NH_3 (Zhao et al., 2012). A previous study has shown that the NH_3 concentrations in this region were very high, with annual average concentrations of 21.4, 31.9, and 27.7 ppbv in Quzhou, Shouguang, and Wuqiao, respectively (Shen et al., 2011, with locations shown in Fig. 1b). Both the emissions and the concentration of NH_3 in the summer were highest of any of the four seasons of the year (Meng et al., 2010).

Online instruments were installed in a steel container, with sampling inlets crossing the roof vertically (~4 m a.g.l.). The field campaign was conducted from June 1 to 30, June, 2013. In this study, only data during June 18 to June 30 were used to research the atmospheric chemical processes of fine nitrate formation because the data of fine nitrate in the first half of the month were significantly affected by biomass burning.
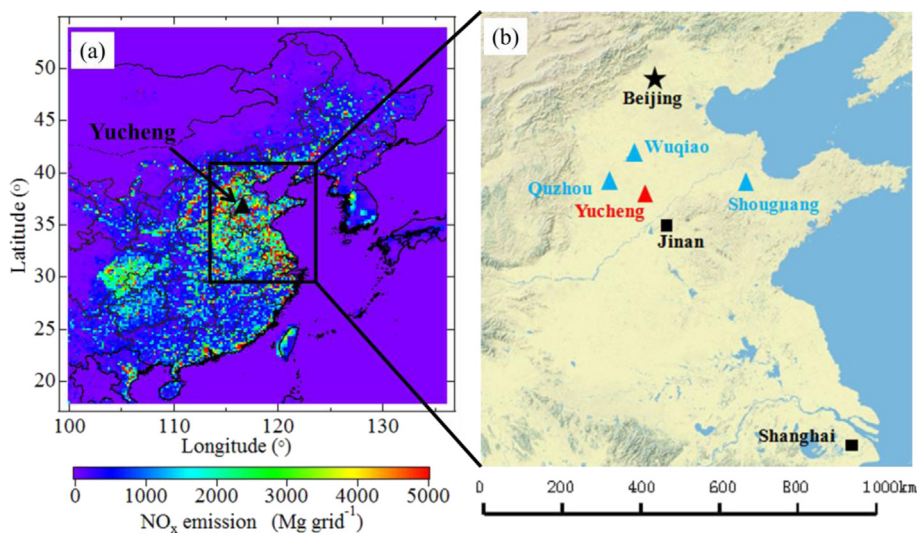
Fig. 1. (a) Location in of the measurement site of Yucheng with colour showing the emission intensity of NO_x in 2006 (Zhang et al., 2009), (b) topographic map of the study region which shows the locations of Yucheng site in this study (marked in red) and some other rural sites in literature (marked in blue). (For interpretation of the references to colour in this figure legend, the reader is referred to the web version of this article.)

2.2. Instruments

In this study, a Monitor for Aerosols and Gases (MARGA, ADI20801, Applikon-ECN, Netherlands) was deployed to continuously measure the concentrations of acid and alkaline gases and inorganic water-soluble ions in $PM_{2.5}$ with a time resolution of 1 h. The flow rate was 16.7 L min^{-1}. The water-soluble gases, including HCl, HNO$_2$, HNO$_3$, SO$_2$, and NH$_3$, were collected by a WRD (Wet Rotating Denuder), and the inorganic water-soluble ions in $PM_{2.5}$, including Cl$^-$, NO$_3^-$, SO$_4^{2-}$, Na$^+$, NH$_4^+$, K$^+$, Mg^{2+} and Ca^{2+}, were collected by a SJAC (Steam Jet Aerosol Collector). These substances were dissolved in the absorption solution (DI water with 15 ppmv H$_2$O$_2$) and were analysed by ion chromatography. The cationic eluent and the anionic eluent were prepared by methanesulphonic acid (308 mg L^{-1}) and NaHCO$_3$ (672 mg L^{-1}) − Na$_2$CO$_3$ (742 mg L^{-1}), respectively. A solution of 4.0 mg L^{-1} LiBr as an internal standard was periodically injected and mixed with the sample solutions for subsequent detection. The detection limits of HCl, HNO$_2$, HNO$_3$, SO$_2$, NH$_3$, Cl$^-$, NO$_3^-$, SO$_4^{2-}$, Na$^+$, NH$_4^+$, K$^+$, Mg^{2+} and Ca^{2+} are 0.00614, 0.0238, 0.00711, 0.0105, 0.0658 ppbv, 0.01, 0.05, 0.04, 0.05, 0.05, 0.09, 0.06, and 0.1 μg m^{-3}, respectively. Multi-point calibrations of nine water-soluble ions were conducted immediately before and after the campaign.

$PM_{2.5}$ was measured with a particle monitor (Model 5030 SHARP Monitor, Thermo Fisher Scientific, USA), and the hourly average concentrations were quantified by the scattering coefficient of 880 nm light and the absorption coefficient of beta rays. The surface area concentration of aerosols in the range of 5 nm to 1 μm was measured with a Wide-Range Particles Spectrometer (WPS, Model 1000XP, MSP Corporation, USA) with the assumption of all aerosols being spherical. The concentration of NO$_x$ (NO and NO$_2$) was detected by the chemiluminescence method (42C, Thermo Electron Corporation, USA) with a molybdenum oxide catalytic converter. The concentration of O$_3$ was measured by the ultraviolet absorption method (49C, Thermo Electron Corporation, USA). In addition, the meteorological data were measured with an automatic meteorological station (MILOS520, Vaisala, Finland).

2.3. Steady-state predictions

Due to their short lifetimes, the concentrations of the NO$_3$ radical and N$_2$O$_5$ can be predicted by steady-state calculations in the situation that measurement data are lacking (Osthoff et al., 2006). The formation and loss of NO$_3$ and N$_2$O$_5$ are dominated by a series of chemical reactions listed in Table 1. Consequently, the NO$_3$ concentration can be calculated by Eq. (1) (Wang et al., 2014a,b),

$$[NO_3]_{cal.} = \frac{k_1 \cdot [NO_2] \cdot [O_3]}{k_3 \cdot [NO] + j_4 + j_5 + k_6 + k_7 + (k_8 + k_9) \cdot k_{eq} \cdot [NO_2]}$$

(1)

A fast equilibrium exists between N$_2$O$_5$ and its decomposition products, NO$_3$ and NO$_2$. Similarly, the N$_2$O$_5$ concentration can be calculated by Eq. (2) (Wang et al., 2014a,b),

$$[N_2O_5]_{cal.} = k_{eq} [NO_2] \cdot [NO_3]_{cal.}$$

(2)

In this study, to help elucidate the contribution of N$_2$O$_5$ hydrolysis to nitrate formation, Eq. (1) and Eq. (2) were used to calculate the steady-state concentrations of NO$_3$ and N$_2$O$_5$. The involved reactions and rate constants together with their provenances are included in Table 1. Due to the lack of VOC measurement data, the total reaction rates of NO$_3$ with VOCs were assumed to be equal to the NO$_3$ loss rate caused by the heterogeneous hydrolysis of N$_2$O$_5$ (Aldener et al., 2006). For the heterogeneous processes on wet aerosol surfaces, the uptake coefficients of the NO$_3$ radical and N$_2$O$_5$ (γ_{NO_3} and $\gamma_{N_2O_5}$) used in this study were 0.004 and 0.03, respectively (Aldener et al., 2006).

3. Results and discussion

3.1. High levels of fine particulate nitrates

3.1.1. Statistic results and comparison with other locations

The concentrations of major water-soluble ions in $PM_{2.5}$ at the Yucheng site and other locations in the summertime are listed in Table 2. At the Yucheng site, the average concentrations (±standard deviations) of $PM_{2.5}$, NO$_3^-$, SO$_4^{2-}$, and NH$_4^+$ were 155.9 (±88.4), 22.5 (±18.6), 28.7 (±17.7), and 18.2 (±11.9) μg m^{-3}, respectively. The fine particulate nitrate concentration exhibited a large variation, ranging from 1.5 to 87.2 μg m^{-3}. The average ratios of NO$_3^-$/PM$_{2.5}$ and NO$_3^-$/SO$_4^{2-}$ were 0.14 (range, 0.014−0.45) and 0.79 (range, 0.06−2.9), respectively. When compared to other locations, the fine particulate nitrate concentration at the Yucheng site is found to be extremely high. The average concentration of fine particulate nitrate at Yucheng was close to those in urban Jinan, four times higher than those in urban Fuzhou and one to six times higher than those observed at rural or suburban sites in Beijing, Shanghai, Lanzhou, and Guangzhou (Pathak et al., 2009; Gao et al., 2011; Zhang et al., 2013). Furthermore, the fine particulate nitrate concentration at Yucheng was dozens of times higher than those measured at urban or rural-coastal sites in Japan and Europe (Khan et al., 2010; Squizzato et al., 2012). The NO$_3^-$/PM$_{2.5}$ ratio at Yucheng was close to that in Beijing and much higher than those at other sites both domestic and abroad. The NO$_3^-$/SO$_4^{2-}$ ratio was much higher than those at all sites listed in Table 2. The results of the elevated fine particulate nitrate concentrations and the very high ratios of NO$_3^-$/PM$_{2.5}$ and NO$_3^-$/SO$_4^{2-}$ at the Yucheng site demonstrate severe fine particulate nitrate pollution in this region.

3.1.2. Time series of fine particulate nitrate concentration

The time dependence of the concentrations of $PM_{2.5}$, NO$_3^-$, together with meteorological parameters and NR (NR = [NH$_4^+$]/(2 [SO$_4^{2-}$] + [NO$_3^-$])) from June 18 to June 30 are shown in Fig. 2. The four highest concentration peaks of NO$_3^-$ in $PM_{2.5}$ were 73.7, 64.9, 82.9, and 87.2 μg m^{-3}, which appeared in the early morning of June 19, 20, 24, and 25, respectively (marked as the red arrows in Fig. 2). The variation pattern of fine particulate nitrate concentration

Table 1
Major chemical reactions involved in NO$_3$ and N$_2$O$_5$ and the reaction rate constants.

Reaction	Reaction rate constant	Provenance
(R1) NO$_2$ + O$_3$ → NO$_3$ + O$_2$	k_1	a, b
(R2) NO$_3$ + NO$_2$ ↔ N$_2$O$_5$	K_{eq}	a, b
(R3) NO$_3$ + NO → NO$_2$ + NO$_2$	k_3	a, b
(R4) NO$_3$ → NO$_2$ + O	j_4	c
(R5) NO$_3$ → NO + O$_2$	j_5	c
(R6) NO$_3$ $\xrightarrow{VOC}$ products	$k_6 = \sum(k_{VOC,i} \cdot [VOC]_i)$	b
(R7) NO$_3$ $\xrightarrow{Heterogeneous}$ products	$k_7 = \frac{1}{4} \cdot C_{NO_3} \cdot \gamma_{NO_3} \cdot S_{aerosol}$	d, e
(R8) N$_2$O$_5$ $\xrightarrow{Heterogeneous}$ products	$k_8 = \frac{1}{4} \cdot C_{N_2O_5} \cdot \gamma_{N_2O_5} \cdot S_{aerosol}$	e, f
(R9) N$_2$O$_5$ $\xrightarrow{Homogeneous}$ 2HNO$_3$	$k_9 = k_I \cdot [H_2O] + k_{II} \cdot [H_2O]^2$	g

[a] Master Chemical Mechanism (MCM version 3.1 http://mcm.leeds.ac.uk/MCM/) (Saunder et al., 2006).
[b] Atkinson and Arey, 2003.
[c] Calculated as functions of solar zenith angles (MCM).
[d] Evans and Jacob, 2005.
[e] Aldener et al., 2006.
[f] Osthoff et al., 2006.
[g] Wahner et al., 1998.

Table 2
Concentrations of $PM_{2.5}$ and secondary water-soluble inorganic ions at Yucheng and other sites during summer in domestic and abroad in recent years.

Site	Types of study sites	Measurement periods	$PM_{2.5}$ ($\mu g\ m^{-3}$)	NO_3^- ($\mu g\ m^{-3}$)	SO_4^{2-} ($\mu g\ m^{-3}$)	NH_4^+ ($\mu g\ m^{-3}$)	$NO_3^-/PM_{2.5}$	NO_3^-/SO_4^{2-}	Provenance
Yucheng, China (Min.)	Rural	Jun. 2013	48.9	1.5	3.7	4.2	0.014	0.06	This study
Yucheng, China (ave.)			155.9	22.5	28.7	18.2	0.14	0.79	
Yucheng, China (max.)			356.2	87.2	99.7	54.9	0.45	2.9	
Beijing, China	Rural	Jun.–Aug. 2005	68	9.9	22.6	4.7	0.15	0.44	Pathak et al., 2009
Shanghai, China	Suburban	May–Jun. 2005	67	7.1	15.8	4.1	0.11	0.45	
Lanzhou, China	Suburban	Jun.–Jul. 2006	65	3.2	9.8	4.1	0.049	0.33	
Guangzhou, China	Suburban	May 2006	55	5.2	13.1	4.8	0.1	0.4	
Fuzhou, China	Urban	Sept. 2007	69.5	5.6	14.4	5.9	0.080	0.39	Zhang et al., 2013
Jinan, China	urban	Jun. 2008	173.2	19.2	64.3	28.0	0.11	0.3	Gao et al., 2011
Yokohama, Japan	urban	Jun.–Aug. 2008	20.8	0.2	4.6	4.4	0.008	0.037	Khan et al., 2010
Punta Sabbioni, Europe	rural-coastal	Jun.–Jul. 2009	11	0.5	2.4	1	0.045	0.21	Squizzato et al., 2012
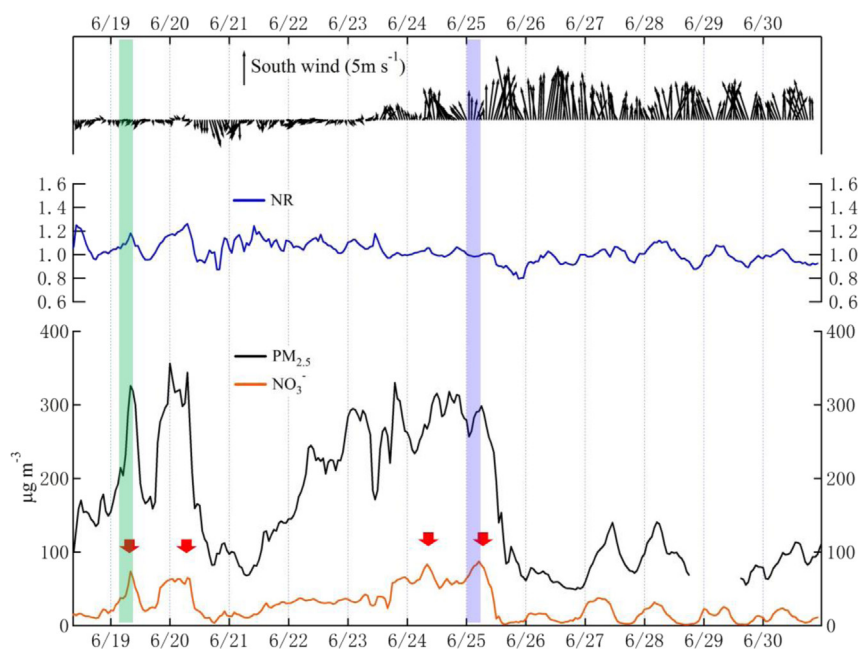
Fig. 2. Time series of concentrations of NO_3^-, $PM_{2.5}$, wind direction, wind speed, and NR (NR = $[NH_4^+]/(2[SO_4^{2-}] + [NO_3^-])$) at Yucheng site from June 18 to June 30, 2013. Four serious polluted cases of fine particulate nitrate were noted by red arrows. The green and blue shadows show two typical cases and will be discussed in 3.2 and 3.3, respectively. (For interpretation of the references to colour in this figure legend, the reader is referred to the web version of this article.)

tracked well with that of $PM_{2.5}$ (slope = 0.19 and R^2 = 0.72 for the data during periods from 20:00 to 7:00 the next morning).

It is well-known that the formation of fine particulate nitrate largely depends on meteorological conditions and the mixing ratios of precursors and oxidants. During the measurement period, the wind direction and speed were relatively stable, with a low northerly wind speed (1.5 m s^{-1} on average) before June 23 and high southerly wind speed (4.2 m s^{-1} on average) after June 24.

At the Yucheng site, the NH_3 concentration was notably high. The highest, average, and night-time average (20:00–7:00 the next morning) concentrations of NH_3 at the Yucheng site were 120.7, 34.9, and 34.3 ppbv, respectively, much higher than the summer mean value (13.9 ppbv) which was detected at a rural site nearby several swine production facilities in eastern North Carolina, USA (Robargea et al., 2002). During the night-time, more than 59.5% of the NH_3 concentrations were above 30 ppbv and the average value of NR reached 1.09. In addition, the O_3 was also observed at high levels. The maximum, average and night-time average concentrations of O_3 were 175.5, 65.4, and 41.9 ppbv, respectively. During the night-time, more than 65.9% of the ozone concentrations exceeded

40 ppbv. The detailed effects of NH_3 and O_3 on night-time fine particulate nitrate formation will be discussed later.

3.1.3. Diurnal variation of fine particulate nitrates

The average diurnal variations of concentrations of fine particulate nitrate, HNO_3, NH_3, NO_2, O_3, and the $NO_3^-/PM_{2.5}$ ratio from June 18 to June 30, 2013 are shown in Fig. 3. The fine particulate NO_3^- concentration and $NO_3^-/PM_{2.5}$ ratio generally increased gradually during the night-time and decreased during the daytime. The average concentration of fine particulate NO_3^- showed a peak of 34.7 $\mu g\ m^{-3}$ at 7:00 in the early morning, accounting for 22.3% of $PM_{2.5}$. The valley concentration of 12.3 $\mu g\ m^{-3}$ appeared at 16:00, representing a fraction of 9.1% of $PM_{2.5}$.

NO_2, the major primary precursor of nitrate, showed a peak concentration of 23.9 ppbv at 9:00 in the morning. During the night-time, the NO_2 concentration remained high, only a little lower than that during the daytime. The valley concentration of NO_2 reached 14.2 ppbv, appearing at 23:00. Gaseous HNO_3 is readily converted to particulate nitrate via reaction with NH_3 and/ or heterogeneous uptake on surfaces of alkaline aerosols or small
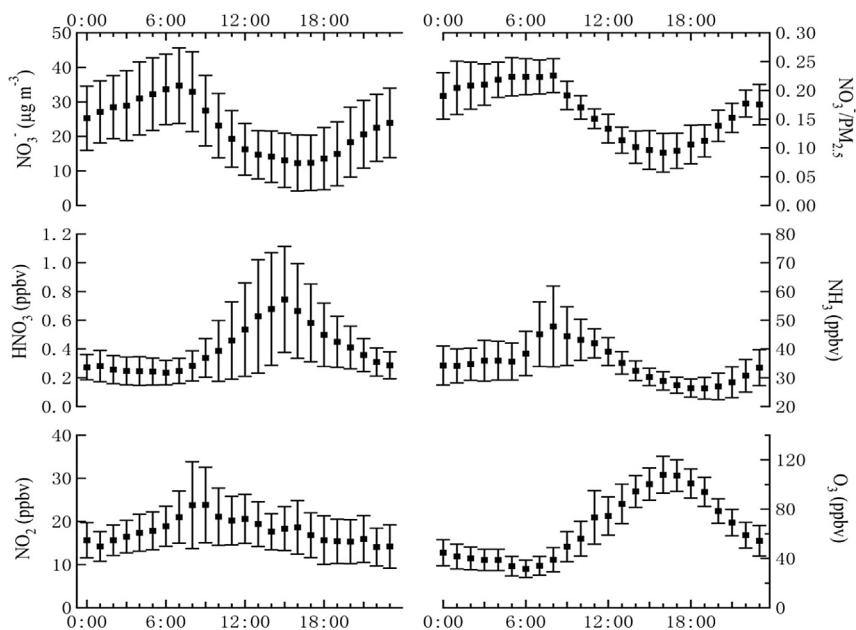
Fig. 3. Average diurnal variations of concentrations of fine particulate nitrates, HNO₃, NH₃, NO₂, O₃, and NO₃⁻/PM₂.₅ ratio at Yucheng for the period from June 18 to June 30, 2013. The standard deviations are presented as the error bars.

droplets. The HNO_3 concentration was relatively low, showing a maximum average concentration of 0.75 ppbv at 15:00. Surprisingly, the NH_3 concentration was quite high at the Yucheng site, exhibiting a peak of 47.9 ppbv appearing at 8:00 in the morning. O_3, one of the most important oxidants, exhibited a large concentration peak in the afternoon with maximum value of 107.8 ppbv at 16:00. This very high O_3 concentration demonstrates that the study region experienced serious photochemical pollution. The night-time O_3 concentration remained high (e.g., 44.6 ppbv at 0:00), indicating a relatively strong oxidation capacity, even at night.
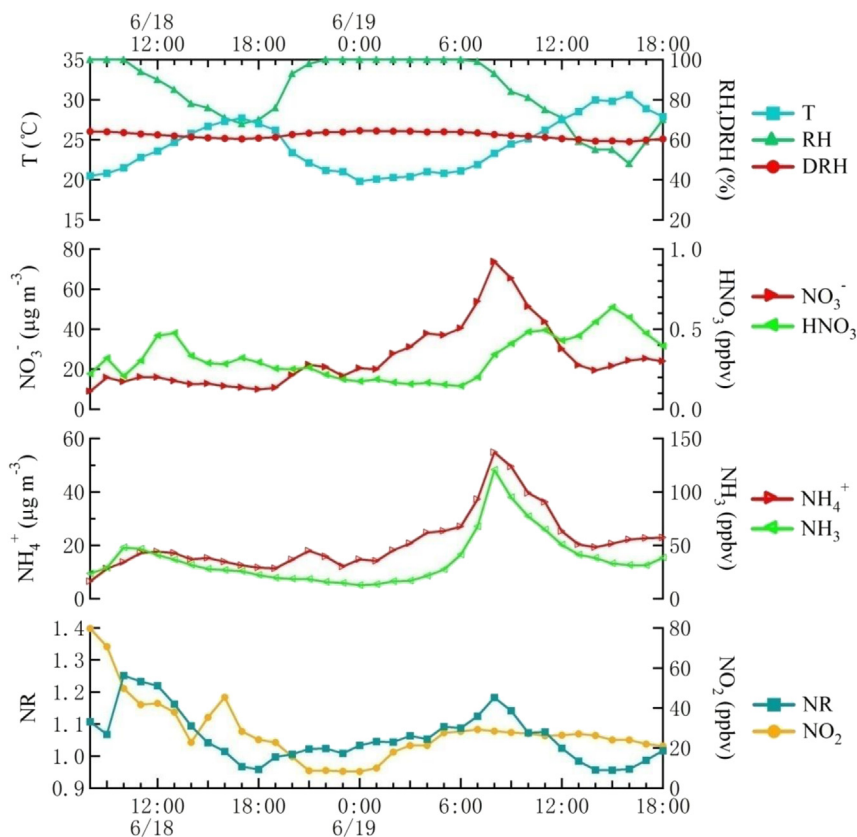
Fig. 4. Time series of meteorological data and the concentrations of air pollutants related to nitrate formation on June 18 and June 19.

3.2. Fine particulate nitrate formation associated with ammonia

In the early morning of June 19, elevated concentrations of fine particulate NO_3^- were observed and the simultaneous NH_3 concentrations were very high (as shown in Fig. 4). This case was selected to analyse the detailed impact of NH_3 on fine particulate nitrate formation. Within the 4 h before 8:00 on June 19, the mass concentration of fine particulate NO_3^- increased by a factor of 2.0 from 37.0 to 73.7 $\mu g\ m^{-3}$ and the $PM_{2.5}$ concentration rose by a factor of 1.6 from 203.8 $\mu g\ m^{-3}$ to 325.8 $\mu g\ m^{-3}$. The increase in fine particulate nitrate concentration tracked the NH_3 concentration well, which rose from 27.4 ppbv to 120.7 ppbv. During this period, the $\Delta NO_3^-/\Delta PM_{2.5}$ ratio was 0.30, higher than the $\Delta SO_4^{2-}/\Delta PM_{2.5}$ of 0.27 and the $\Delta NH_4^+/\Delta PM_{2.5}$ ratio of 0.24, suggesting that the fine particulate nitrate formation obvious contributed to $PM_{2.5}$ pollution in this case. The NH_4^+ concentration increased from 25.3 $\mu g\ m^{-3}$ to 54.9 $\mu g\ m^{-3}$ and the NR value rose from 1.09 to 1.18, but the concentrations of other inorganic ions were very low, indicating that the newly produced fine particulate nitrate existed mainly in the form of NH_4NO_3. The enhancement of NH_4^+ together with the increase in NR indicates that large amount of NH_3 anticipated the fine nitrate formation and thus played an important role in the rapid accumulation of fine particulate nitrate. During this period, the ambient RH was substantially higher than the DRH (deliquescence relative humidity of NH_4NO_3, DRH $= e^{((723.7/T)+1.6954)}$, Lin et al., 2007) during this period. Therefore, the fine particulate nitrate mainly dissolved in small droplets or in water on aerosol surfaces.

Assuming that solid or aqueous NH_4NO_3 in aerosols was in equilibrium with its gaseous precursors of HNO_3 and NH_3, the fine nitrate quantitative relationship between concentrations of them can be expressed by a series of equations (Lin and Cheng, 2007). In this study, the concentration of NH_4NO_3 was also calculated based on the observed concentrations of HNO_3 and NH_3. However, the average calculated fine nitrate concentration (0.58 $\mu g\ m^{-3}$) was much lower than that observed average value (51.2 $\mu g\ m^{-3}$) within the 4 h before 8:00 in June 19. This discrepancy demonstrates that the ammonia-associated elevated concentration of fine nitrate possibly formed in other locations and transported to our measurement site. This finding also indicates the complexity of fine nitrate formation, and further in-depth studies are warranted. In addition, the average O_3 concentration was only 22.1 ppbv between 5:00 and 8:00 in June 19, which provides further evidence that NH_3, not the photochemical reaction, was the main factor to promote the fine nitrate formation in this case.

NR is an important parameter to represent the relative abundance of NH_4^+ and the participation of NH_3 in fine nitrate formation. For cases with and without increasing NR, scatter plots of NO_3^- in $PM_{2.5}$ and NH_3 during the periods from 20:00 to 7:00 the next morning were shown in Fig. 5a and b, respectively. When NR rose, the fine particulate NO_3^- concentration tracked well with NH_3 concentration (slope = 0.82, $R^2 = 0.582$, six nights), suggesting that NH_3 was the major factor causing the fine nitrate formation during these periods. However, the NO_3^- concentrations did not change with NH_3 concentrations ($R^2 = 0.003$, six nights) if the NR did not increase, indicating that in these nights the fine nitrate formation might be dominated by other factors.

3.3. Fine particulate nitrate formation related to ozone

During the period from the evening of June 24 to the early morning of June 25, fast nitrate formation was observed to be accompanied by high concentrations of O_3 (see Fig. 6). Within the 10 h before 21:00 in June 24, the average concentration of fine NO_3^- was as high as 57.4 $\mu g\ m^{-3}$. Surprisingly, the fine NO_3^- concentration further increased after 21:00 and reached to an extremely high level of 87.2 $\mu g\ m^{-3}$ at 5:00 in June 25. When the maximum NO_3^- concentration appeared, the NO_3^- accounted for a very large fraction of 29.9% in $PM_{2.5}$, ~50% higher than SO_4^{2-}. The fine NO_3^- concentration increased at a fast rate. The average and the maximum rates of increase of fine NO_3^- within the 8 h before 5:00 were 3.7 $\mu g\ m^{-3}\ h^{-1}$ and 7.1 $\mu g\ m^{-3}\ h^{-1}$ (appeared at 2:00 in June 25), respectively. At the same time, high concentrations of night-time O_3 were observed. The O_3 concentration was in a high level of 106.5 ppbv at 18:00 in June 24 and was gradually dropped to 41.8 ppbv at 6:00 in June 25, demonstrating strong oxidation capacity in the whole night. Moreover, the ambient RH kept obviously higher than the DRH during the whole night, indicating that nitrate primarily deliquesced on the surfaces of wet aerosols or small droplets.

Within the 8 h before 5:00 on June 25, the NH_3 concentration did not show any obvious increase and the NR value kept decreasing, which is significantly different from the other cases of enhanced fine nitrate formation associated with NH_3. During the period from 21:00 on June 24 to 5:00 on June 25, the concentration of SO_4^{2-} in $PM_{2.5}$ did not increase and the NH_4^+ concentration showed no obvious variation. Therefore, the decrease of NR was attributed to new formation of NO_3^- (not SO_4^{2-}) and the NH_3 did not anticipate the fine nitrate formation in this case.
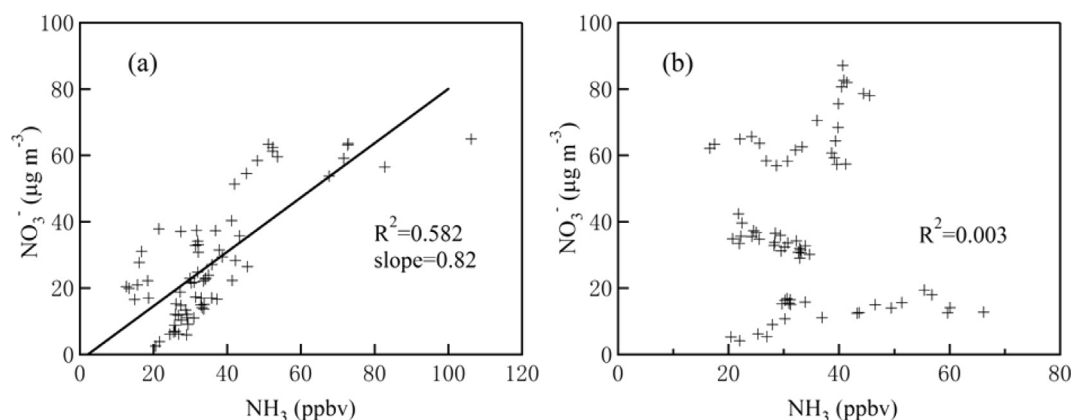
Fig. 5. Scatter plots of hourly concentrations of NO_3^- and NH_3 during periods from 20:00 to 7:00 in the next morning for cases (a) with and (b) without increasing NR. The data were selected from June 18 to June 20 and from June 26 to June 30 for the left plot and from June 20 to 26 for the right plot.
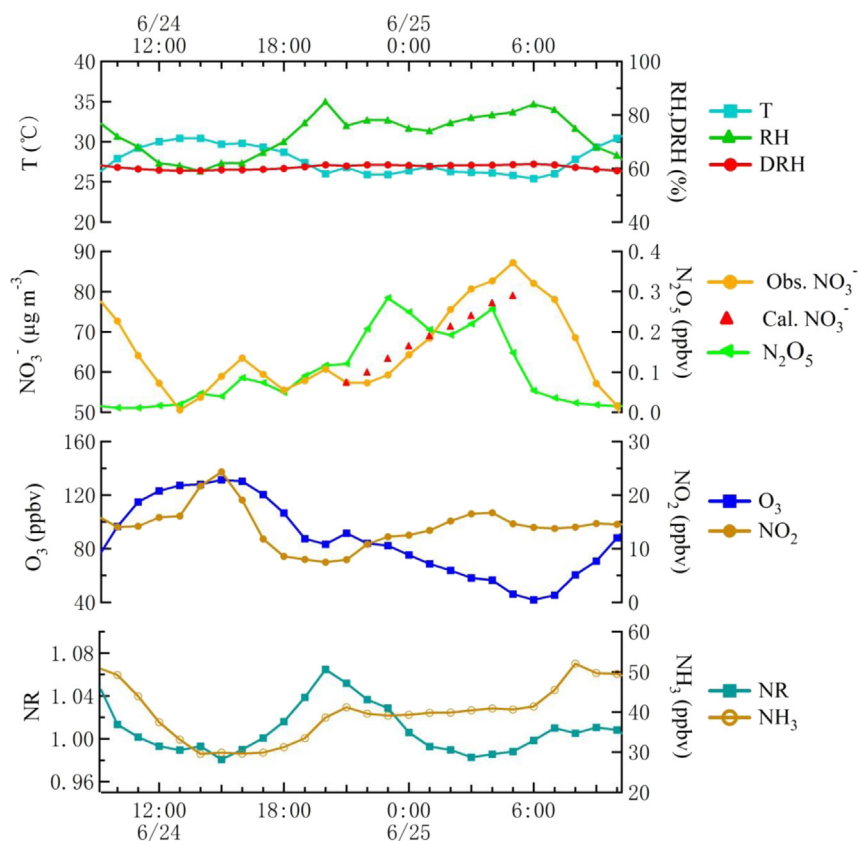
Fig. 6. Time series of meteorological data and the concentrations of air pollutants related to nitrate formation from June 24 to June 25.

In this study, the N_2O_5 concentrations were calculated by using steady-state expressions from 10:00 on June 24 to 9:00 on June 25 and are shown in Fig. 6. The calculated N_2O_5 concentrations also exhibited a large peak from 21:00 on June 24 to 5:00 on June 25 with a maximum hourly concentration of 0.28 ppbv. The fine nitrate concentration of 57.4 $\mu g\ m^{-3}$ at 21:00 on June 24 was selected as the initial concentration of the calculated concentration within 8 h after 21:00 on June 24. Hence the calculated NO_3^- concentration in the 8 h period (as shown in Fig. 6) can be calculated by adding the increase in fine nitrate concentration from N_2O_5 hydrolysis during each hour. The calculated NO_3^- concentration of 79.0 $\mu g\ m^{-3}$ at 5:00 on June 25 was very close to the observed NO_3^- peak concentration of 87.2 $\mu g\ m^{-3}$. Furthermore, the average increase rate of the calculated NO_3^- from the N_2O_5 hydrolysis was 2.7 $\mu g\ m^{-3}\ h^{-1}$, close to that of the observed NO_3^- rate (3.7 $\mu g\ m^{-3}\ h^{-1}$). These results suggest that the heterogeneous hydrolysis of N_2O_5 on wet aerosol surfaces was the major formation pathway for the fast fine nitrate formation in this case.

To further understand the impact of O_3 on night-time nitrate formation, the data with high night-time NO_3^- concentration peaks (excluding days when it was raining) were selected to perform a correlation analysis. Fig. 7 shows the scatter plot of the average increase rate of fine NO_3^- versus the average O_3 concentration during periods with obvious night-time fine nitrate formation. The increase rate of NO_3^- strongly correlated and rose positively with the average O_3 concentration ($R^2 = 0.783$, slope = 0.038). This suggests that hydrolysis of N_2O_5 is one of the major formation pathways of fine nitrate and significantly contributed to the elevated fine nitrate concentrations at night-time during summer in rural areas in the North China Plain.

4. Summary and conclusions

Online measurements of fine particulate nitrate, related air pollutants and meteorological parameters were conducted from June 18 to June 30, 2013 at a rural site on the North China Plain, where a large amount of ammonia was emitted, and severe photochemical pollution frequently appeared during the summer. During the measurement period, notably high levels of fine nitrate were usually observed from the evening to the next morning, with a maximum hourly concentration of 87.2 $\mu g\ m^{-3}$ appearing at 5:00
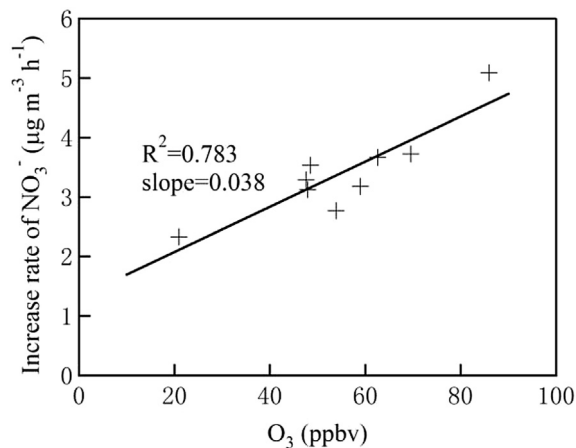
Fig. 7. Scatter plot of increase rate of fine NO_3^- and the average night-time O_3 concentration during the periods with fine nitrate formation from June 18 to June 20 and from June 23 to June 30.

on June 25. The observed nitrate accounted for a large fraction of $PM_{2.5}$, ranging from 1.4 % to 45 % (an average of 14%). Subsequent case analyses and data calculations suggest that the elevated fine nitrate concentration and the fast nitrate formation were strongly related to the high levels of NH_3 and O_3 in the study area. In a number of cases, the concentration peak of fine particulate nitrate appeared exactly at the same time when the NH_3 concentration exhibited a peak. Extremely high concentrations of NH_3 (120.7 ppbv in maximum) anticipated the fine particulate nitrate formation and led to a rising neutralization ratio. In some other cases, the fast secondary formation of fine nitrate was attributed to the hydrolysis of N_2O_5 which was produced from the reaction of high concentrations of night-time O_3 with moderate levels of NO_2. The calculated N_2O_5 concentrations via steady-state expressions and the resulting nitrate formation rate are generally consistent with the observed nitrate formation. The heterogeneous hydrolysis of N_2O_5 on wet aerosol surfaces resulted in elevated fine nitrate concentrations and a reduced neutralization ratio. Considering the important roles that high levels of NH_3 and O_3 play in the enhanced nitrate formation, control measures are suggested to reduce the emissions of NH_3 and ozone precursors (i.e., NO_x and VOCs) to address the serious occurrence of $PM_{2.5}$ pollution on the North China Plain.

Acknowledgements

References

Aldener, M., Brown, S.S., Stark, H., Williams, E.J., Lerner, B.M., Kuster, W.C., Goldan, P.D., Quinn, P.K., Bates, T.S., Fehsenfeld, F.C., Ravishankara, A.R., 2006. Reactivity and loss mechanisms of NO_3 and N_2O_5 in a polluted marine environment: result from in situ measurements during New England Air Quality Study 2002. J. Geophys. Res. 111, D23S73.

Atkinson, R., Arey, J., 2003. Atmospheric degradation of volatile organic compounds. Chem. Revel. 103, 4605–4638.

Calvert, J.G., Stockwell, W.R., 1983. Acidic generation in the troposphere by gas phase chemistry. Environ. Sci. Technol. 17, 428–443.

Carslaw, D.C., Rhys-Tyler, G., 2013. New insights from comprehensive on-road measurements of NO_x, NO_2 and NH_3 from vehicle emission remote sensing in London, UK. Atmos. Environ. 81, 339–347.

Du, H.H., Kong, L.D., Cheng, T.T., Chen, J.M., Du, J.F., Li, L., Xia, X.G., Leng, C.P., Huang, G.H., 2011. Insights into summertime haze pollution events over Shanghai based on online water-soluble ionic composition of aerosols. Atmos. Environ. 45, 5131–5137.

Evans, M.J., Jacob, D.J., 2005. Impact of new laboratory studies of N_2O_5 hydrolysis on global model budgets of tropospheric nitrogen oxides, ozone, and OH. Geophys. Res. Lett. 32, 1–4.

Feng, Y., Penner, J.E., 2007. Global modeling of nitrate and ammonium: interaction of aerosols and tropospheric chemistry. J. Geophys. Res. 112, D1.

Gao, X.M., Yang, L.X., Cheng, S.H., Gao, R., Zhou, Y., Xue, L.K., Shou, Y.P., Wang, J., Wang, X.F., Nie, W., Xu, P.J., Wang, W.X., 2011. Semi-continuous measurement of water-soluble ions in $PM_{2.5}$ in Jinan, China: temporal variations and source apportionment. Atmos. Environ. 45, 6048–6056.

Guo, S., Hu, M., Wang, Z.B., Slanina, J., Zhao, Y.L., 2010. Size-resolved aerosol water-soluble ionic compositions in the summer of Beijing: implication of regional secondary formation. Atmos. Chem. Phys. 10, 947–959.

Hu, D.W., Chen, J.M., Ye, X.N., Li, L., Yang, X., 2011. Hygroscopicity and evaporation of ammonium chloride and ammonium nitrate: relative humidity and size effects on the growth factor. Atmos. Environ. 45, 2349–2355.

Khan, M.F., Shirasuna, Y., Hirano, K., Masunaga, S., 2010. Characterization of $PM_{2.5}$, $PM_{2.5-10}$ and PMN_{10} in ambient air, Yokohama, Japan. Atmos. Res. 96, 159–172.

Lei, H., Wuebbles, D.J., 2013. Chemical competition in nitrate and sulfate formations and its effect on air quality. Atmos. Environ. 80, 472–477.

Lin, Y.C., Cheng, M.T., 2007. Evaluation of formation rates of NO_2 to gaseous and particulate nitrate in the urban atmosphere. Atmos. Environ. 41, 1903–1910.

Liu, X.J., Zhang, Y., Han, W.X., Tang, A.H., Shen, J.L., Cui, Z.L., Peter, V., Jan, W.E., Keith, G., Peter, C., Andreas, F., Zhang, F.S., 2013. Enhanced nitrogen deposition over China. Nature 28, 459–463.

Luo, X.S., Liu, P., Tang, A.H., Liu, J.Y., Zong, X.Y., Zhang, Q., Kou, C.L., Zhang, L.J., Fowler, D., Fangmeier, A., Christie, P., Zhang, F.S., Liu, X.J., 2013. An evaluation of atmospheric Nr pollution and deposition in North China after the Beijing Olympics. Atmos. Environ. 74, 209–216.

Meng, Z.Y., Xu, X.B., Wang, T., Zhang, X.Y., Yu, X.L., Wang, S.F., Lin, W.L., Chen, Y.Z., Jiang, Y.A., An, X.Q., 2010. Ambient sulphur dioxide, nitrogen dioxide, and ammonia at ten background and rural sites in China during 2007–2008. Atmos. Environ. 44, 625–2631.

Mentel, T.F., Bleilebens, D., Wahner, A., 1996. A study of nighttime nitrogen oxide oxidation in a reaction chamber — the fate of NO_2, N_2O_5, HNO_3, and O_3 at different humidities. Atmos. Environ. 30, 4007–4020.

Mozurkewich, M., 1993. The dissociation constant of ammonium nitrate and its dependence on temperature, relative humidity and particle size. Atmos. Environ. 27, 261–270.

Osthoff, H.D., Sommariva, R., Baynard, T., Pettersson, A., Williams, E.J., Lerner, B.M., Roberts, J.M., Stark, H., Goldan, P.D., Kuster, W.C., Bates, T.S., Coffman, D., Ravishankara, A.R., Brown, S.D., 2006. Observation of daytime N_2O_5 in the marine boundary layer during New England Air Quality Study—Intercontinental transport and chemical transformation 2004. J. Geophys. Res. 111, D23S14.

Pathak, R.K., Wu, W.S., Wang, T., 2009. Summertime $PM_{2.5}$ ionic species in four major cities of China: nitrate formation in an ammonia-deficient atmosphere. Atmos. Chem. Phys. 9, 1711–1722.

Pathak, R.K., Wang, T., Wu, W.S., 2011. Nighttime enhancement of $PM_{2.5}$ nitrate in ammonia-poor atmospheric conditions in Beijing and Shanghai: plausible contributions of heterogeneous hydrolysis of N_2O_5 and HNO_3 partitioning. Atmos. Environ. 45, 1183–1191.

Ravishankara, A.R., 1997. Heterogeneous and multiphase chemistry in the troposphere. Science 276, 1058–1065.

Richter, A., Burrows, J.P., Nuß, H., Granier, C., Niemeier, U., 2005. Increase in tropospheric nitrogen dioxide over China observed from space. Nature 437, 129–132.

Robargea, W.P., Walkerb, J.T., McCullochc, R.B., Murrayd, G., 2002. Atmospheric concentrations of ammonia and ammonium at an agricultural site in the southeast United States. Atmos. Environ. 36, 1661–1674.

Saunder, S.P., Golden, D., Kurylo, M., Moortgat, G., Wine, P., Ravishankara, A., Kolb, C., Molina, M., Finlayson-Pitts, B., Huie, R., 2006. Chemical Kinetics and Photochemical Data for Use in Atmospheric Studies. Evaluation Number 17. Jet Propulsion Laboratory, National Aeronautics and Space Administration, Pasadena, CA.

Shen, J.L., Liu, X.J., Zhang, Y., Fangmeier, A., Goulding, K., Zhang, F.S., 2011. Atmospheric ammonia and particulate ammonium from agricultural sources in the North China Plain. Atmos. Environ. 45, 5033–5041.

Shi, Y., Chen, J.M., Hu, D.W., Wang, L., Yang, X., Wang, X.M., 2014. Airborne submicron particulate (PM_1) pollution in Shanghai, China: chemical variability, formation/dissociation of associated semi-volatile components and the impacts on visibility. Sci. Total Environ. 473–474, 199–206.

Squizzol, S., Masiol, M., Innocente, E., Pecorari, E., Rampazzo, G., Pavoni, B., 2012. A procedure to assess localand long-range transport contributions to $PM_{2.5}$ and secondary inorganic aerosol. J. Aerosol Sci. 46, 64–76.

Wahner, A., Mentel, T.F., Sohn, M., 1998. Gas phase reaction of N_2O_5 with water vapor: Importance of heterogeneous hydrolysis of N_2O_5 and surface desorption of HNO_3 in a large Teflon chamber. Geophys. Res. Lett. 25, 2169–2172.

Wang, T., Ding, A.J., Gao, J., Wu, W.S., 2006. Strong ozone production in urban plumes from Beijing, China. Geophys. Res. Lett. 33, L21806.

Wang, T., Nie, W., Gao, J., Xue, L.K., Gao, X.M., Wang, X.F., Qiu, J., Poon, C.N., Meinardi, S., Blake, D., Wang, S.L., Ding, A.J., Chai, F.H., Zhang, Q.Z., Wang, W.X., 2010. Air quality during the 2008 Beijing Olympics: secondary pollutants and regional impact. Atmos. Chem. Phys. 10, 7603–7615.

Wang, X.F., Chen, J.M., Sun, J.F., Li, W.J., Yang, L.X., Wen, L., Wang, W.X., Wang, X.M., Collett Jr., J.L., Shi, Y., Zhang, Q.Z., Hu, J.T., Yao, L., Zhu, Y.H., Sui, X., Sun, X.M., Mellouki, A., 2014a. Severe haze episodes and seriously polluted fog water in Ji'nan, China. Sci. Total Environ. 493, 133–137.

Wang, X.F., Wang, T., Yan, C., Tham, Y.J., Xue, L.K., Xu, Z., Zha, Q.Z., 2014b. Large daytime signals of N_2O_5 and NO_3 inferred at 62 amu in a TD-CIMS: chemical interference or a real atmospheric phenomenon? Atmos. Meas. Technol. 7, 1–12.

Wang, X.F., Zhang, Y.P., Chen, H., Yang, X., Chen, J.M., 2009. Particulate nitrate formation in a highly polluted urban area: a case study by single-particle mass spectrometry in Shanghai. Environ. Sci. Technol. 43, 3061–3066.

Wang, Y., Zhuang, G.S., Tang, A., Yuan, H., Sun, Y., Chen, S., Zheng, A., 2005. The ion chemistry and the source of $PM_{2.5}$ aerosol in Beijing. Atmos. Environ. 39, 3771–3784.

Ye, B., Ji, X., Yang, H., Yao, X., Chan, C.K., Cadle, S.H., Chan, T., Mulawa, P.A., 2003. Concentration and chemical compositions of $PM_{2.5}$ in Shanghai for 1-year period. Atmos. Environ. 37, 499–510.

Ye, X.N., Ma, Z., Zhan, J.C., Du, H.H., Chen, J.M., Chen, H., Yang, X., Gao, W., Geng, F.H., 2011. Important role of ammonia on haze formation in Shanghai. Environ. Res. Lett. 6, 24019–24023.

Zhang, F.W., Xu, L.L., Chen, J.S., Chen, X.Q., Niu, Z.C., Lei, T., Li, C.M., Zhao, J.P., 2013. Chemical characteristics of $PM_{2.5}$ during haze episodes in the urban of Fuzhou, China. Particuology 11, 264–272.

Zhang, H., Shen, Z., Wei, X., Zhang, M., Li, Z., 2012. Comparison of optical properties of nitrate and sulfate aerosol and the direct radiative forcing due to nitrate in China. Atmos. Res. 113, 113–125.

Zhang, Q., Streets, D.G., Carmichael, G.R., He, K.B., Huo, H., Kannari, A., Klimont, Z., Park, I.S., Reddy, S., Fu, J.S., Chen, D., Duan, L., Lei, Y., Wang, L.T., Yao, Z.L., 2009. Asian emissions in 2006 for the NASA INTEX-B mission. Atmos. Chem. Phys. 9, 5131–5153.

Zhao, B., Wang, P., Ma, J.Z., Zhu, S., Pozzer, A., Li, W., 2012. A high-resolution emission inventory of primary pollutants for the Huabei region, China. Atmos. Chem. Phys. 12, 481–501.